Supporting Information for "Fidelity of the coral Sr/Ca paleothermometer following heat stress in the northern Galápagos"

Anson H. Cheung[1], Julia E. Cole[2], Diane M. Thompson[3], Lael Vetter[3],

Gloria Jimenez[4], Alexander W. Tudhope[5]

[1]Department of Earth, Environmental, and Planetary Sciences, Brown University, Providence, RI 02912

[2]Department of Earth and Environmental Sciences, 1100 N. University Ave., University of Michigan, Ann Arbor, MI 48109

[3]Department of Geosciences, 1040 E. 4th St., University of Arizona, Tucson, AZ 85721

[4]Chubb Limited, Philadelphia, PA, 19106

[5]School of Geosciences, University of Edinburgh, Edinburgh, UK

Contents of this file

Corresponding author: A. H. Cheung, Department of Earth, Environmental, and Planetary Sciences, Brown University, Providence, RI 02912. (anson_cheung@brown.edu)

Introduction

This supporting information (SI) contains discussion on the definition of marine heatwaves that could cause coral bleaching, and on different ways to create age-depth models, including their effects on Sr/Ca-SST calibration. This SI also contains SEM and x-ray images, figures related to El Niño and marine heatwaves occurrence, differences in SST datasets, impacts of different age models on Sr/Ca-SST calibration and residual characteristics, running standard deviation of SST and Sr/Ca, and an assessment of data input on the regression slope.

Text S1. Marine Heatwaves

Marine heatwaves have major impacts on marine life and climate, highlighting the importance of understanding how they will change as climate warms. Analyses based on instrumental records and global climate model simulations suggest an increase in frequency and intensity of marine heatwaves due to anthropogenic forcing (e.g. Fröhlicher et al., 2018; Oliver et al., 2018). However, various metrics have been used to define marine heatwaves, which impedes our ability to fully understand the impacts of marine heatwaves on marine ecosystems (Hobday et al., 2016).

The most commonly used metric to associate marine heatwaves with coral bleaching is Degrees Heating Week. This metric is based on a bleaching threshold and is defined as the sum of sea surface temperature (SST) that exceeded a threshold (1°C + maximum mean monthly SST in climatology) over the past 12 weeks (Liu et al., 2003). Similar to this approach, an alternative metric, Degrees Heating Month, is defined to detect coral bleaching events using monthly SST (Donner, 2011). Although these metrics are useful to

detect and predict coral bleaching events, they exhibit high false positive rates (Donner, 2011). Furthermore, the baseline used in these metrics, maximum mean monthly SST in climatology, assumes the maximum SST in each year occurs at the same month. In addition, the threshold assumes corals have a global SST threshold. These conditions have shown to be untrue, especially in the Eastern Equatorial Pacific where the month of maximum SST in each year differs (Donner, 2011). Previous studies have also suggested corals in regions with large natural variability are less susceptible to coral bleaching (Sully et al., 2019; Thompson & van Woesik, 2009). Therefore, we define marine heatwaves using a metric that accounts for variability in the month of maximum SST in each year and that accounts for historical variability (Donner, 2011; Logan et al., 2012).

The availability of satellite data since the 1980s allow for reliable and consistent SST estimates. Hence, it may seem appropriate to use the most recent period to define the marine heatwave metric. However, the most recent period (i.e. ca. 1980 to present) is also marked by high variability and mean SST (Figure S5). As a result, a bleaching threshold based on SST from the most recent period would be high compared to one that used earlier data, and this would underpredict coral bleaching events. Therefore, in this study, we defined the bleaching threshold using gridded data from the earlier part of the instrumental record (1950–1980).

Text S2. Age model and Sr/Ca-SST calibration residual

We developed the age model of our coral records by tying Sr/Ca minima to March SST in each year. This assumes that maximum SST occurs in March of each year and that subannual growth rate is constant. However, we know these are only approximations

(Reed et al., 2021; Wellington & Glynn, 1983). As a result, these assumptions can bias the accuracy of the age model, and thus undermine the strength of the correlation between Sr/Ca and SST.

Since we have reliable observational SST estimates in our analysis period, we can increase the number of tie points and better match Sr/Ca to SST. Specifically, we explore two alternate age models. First, instead of tying Sr/Ca minima to March SST of each year, we tie the Sr/Ca minimum of each year to the observed month of maximum SST, which varies from year to year. This approach accounts for the year-to-year differences in the month of maximum SST. Second, we tie both Sr/Ca minimum and maximum of each year to observed SST maximum and minimum of each year respectively. This approach accounts for both different timing that SST extremes occur and also variable subannual growth rate. Although these two alternate models seem preferable to our approach, they are not possible further back in time when instrumental records are not available.

References

Donner, S. D. (2011). An evaluation of the effect of recent temperature variability on the prediction of coral bleaching events. *Ecological Applications*, *21*(5), 1718-1730. doi: 10.1890/10-0107.1

Fröhlicher, T. L., Fischer, E. M., & Gruber, N. (2018). Marine heatwaves under global warming. *Nature*, *560*(7718), 360–364.

Hobday, A. J., Alexander, L. V., Perkins, S. E., Smale, D. A., Straub, S. C., Oliver, E. C., ... others (2016). A hierarchical approach to defining marine heatwaves. *Progress in Oceanography*, *141*, 227–238.

Liu, G., Strong, A. E., & Skirving, W. (2003). Remote sensing of sea surface temperatures during 2002 barrier reef coral bleaching. *Eos, Transactions American Geophysical Union*, *84*(15), 137–141.

Logan, C. A., Dunne, J., Eakin, C., & Donner, S. (2012). A framework for comparing coral bleaching thresholds. In *Proceedings of the 12th international coral reef symposium (ed yellowlees d, hughes tp), pp 10a3 townsville [internet].*

Oliver, E. C., Donat, M. G., Burrows, M. T., Moore, P. J., Smale, D. A., Alexander, L. V., ... others (2018). Longer and more frequent marine heatwaves over the past century. *Nature communications*, *9*(1), 1–12.

Reed, E. V., Thompson, D. M., Cole, J. E., Lough, J. M., Cantin, N. E., Cheung, A. H., ... Edwards, R. L. (2021). Impacts of coral growth on geochemistry: Lessons from the galápagos islands. *Paleoceanography and Paleoclimatology*, *36*(4), e2020PA004051. doi: https://doi.org/10.1029/2020PA004051

Sully, S., Burkepile, D., Donovan, M., Hodgson, G., & Van Woesik, R. (2019). A global analysis of coral bleaching over the past two decades. *Nature communications*, *10*(1), 1–5.

Thompson, D. M., & van Woesik, R. (2009). Corals escape bleaching in regions that recently and historically experienced frequent thermal stress. *Proceedings of the Royal Society B: Biological Sciences*, *276*(1669), 2893-2901. doi: 10.1098/rspb.2009.0591

Wellington, G. M., & Glynn, P. W. (1983). Environmental influences on skeletal banding in eastern pacific (panama) corals. *Coral reefs*, *1*(4), 215–222.

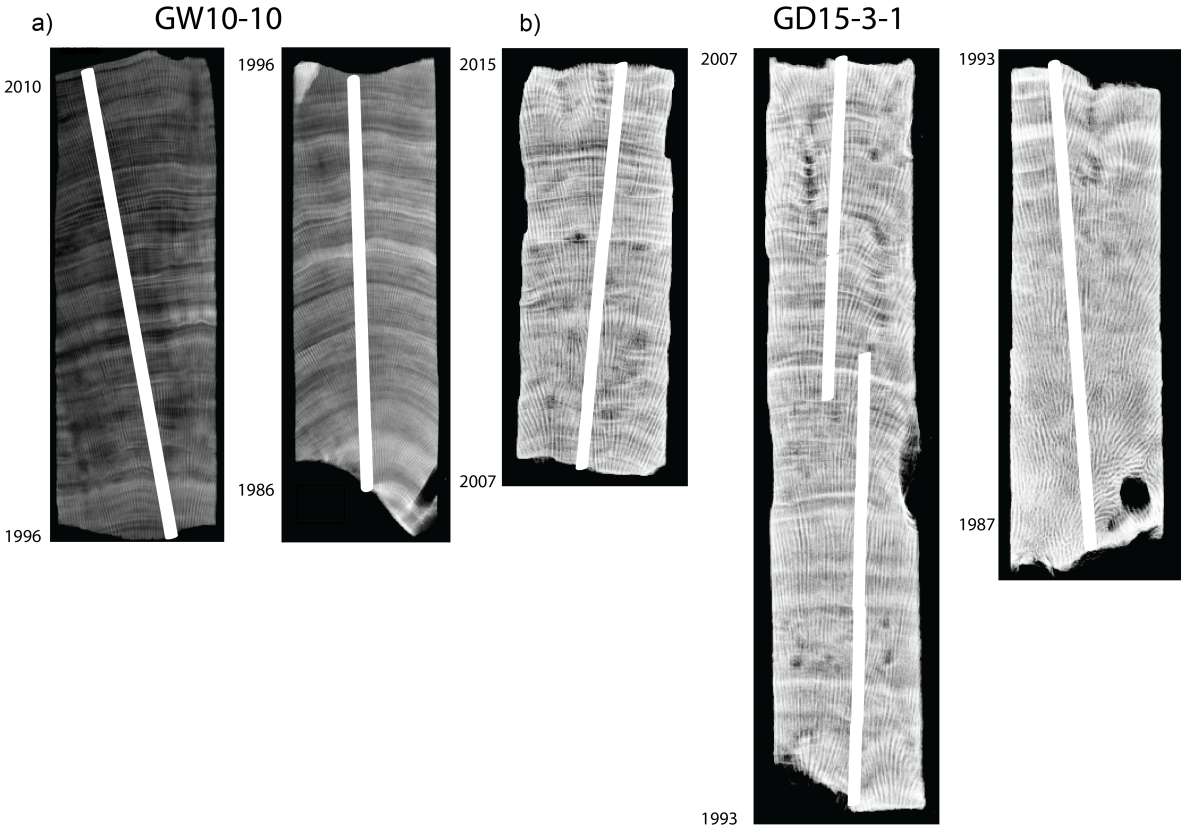

Figure S1. X-ray images of corals, showing sampling transects, from a) GW10-10 and b) GD15-3-1. Topmost sections are on the left in each figure subsection.

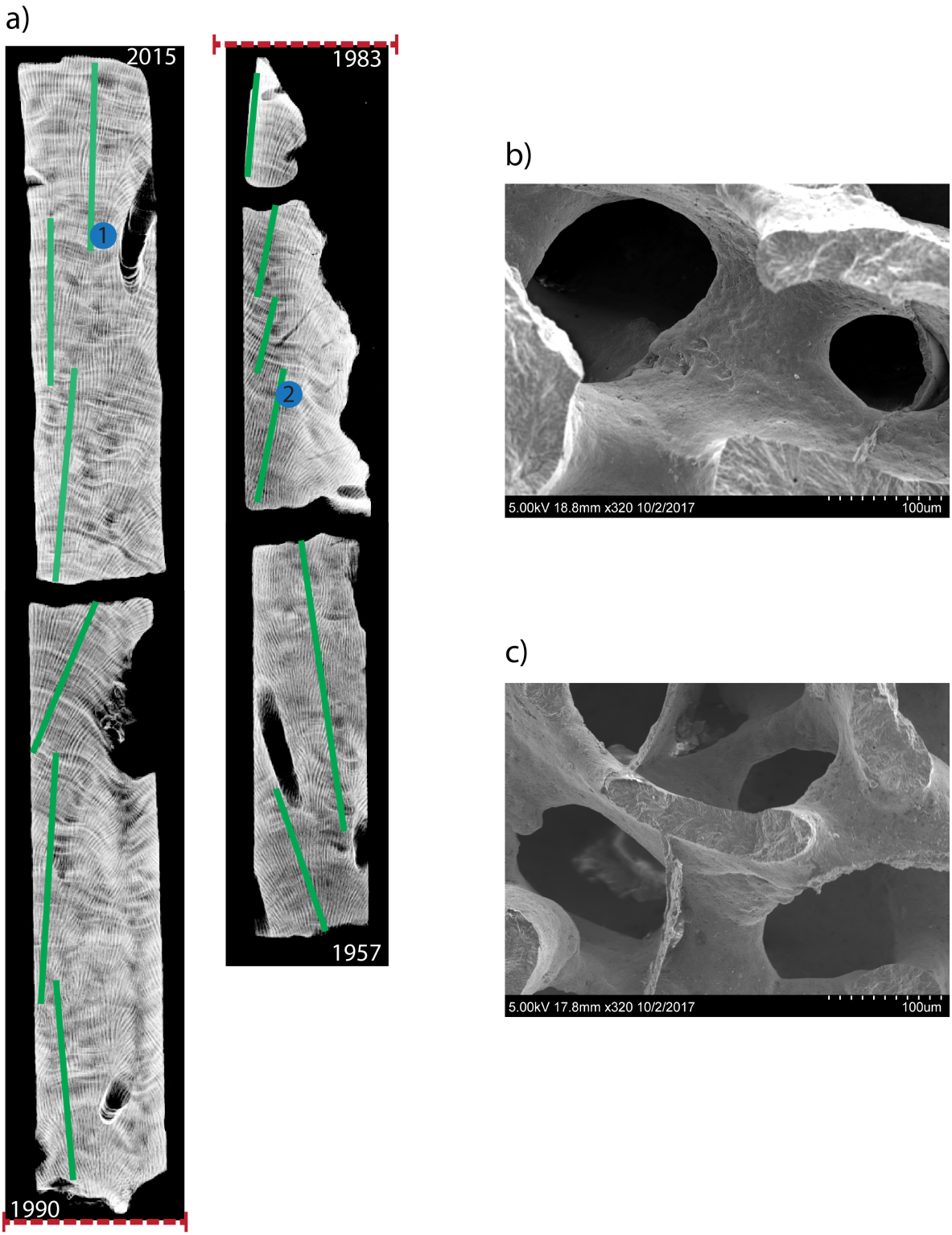

Figure S2. a) X-Ray and b–c) SEM images (b=location 1, c=location 2) of core GD15-3-2. This core was collected from the same coral colony as GD15-3-1. Sampling transects (in green) were not utilized in this study. Red line indicates temporal growth hiatus associated with the 1982-3 El Niño event.

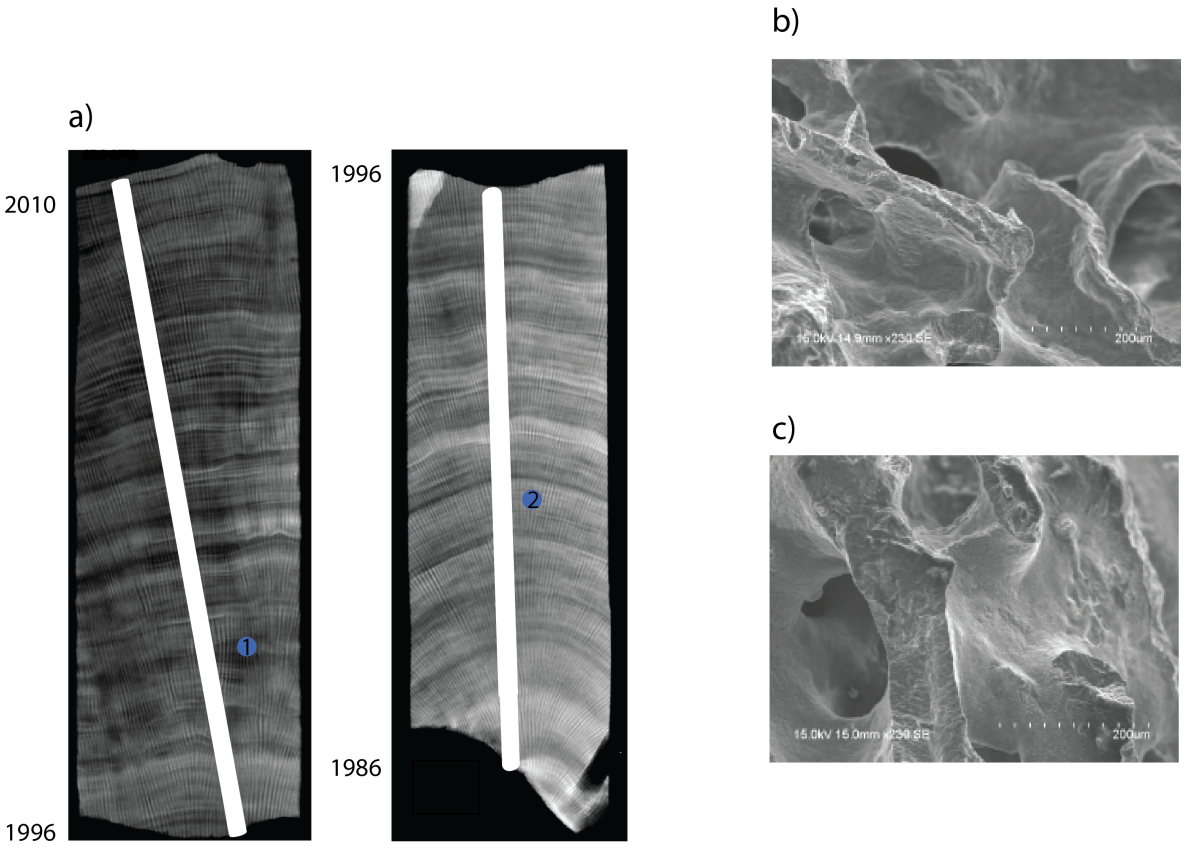

Figure S3. a) X-Ray and b–c) SEM images (b=location 1, c=location 2) from core GW10-10.

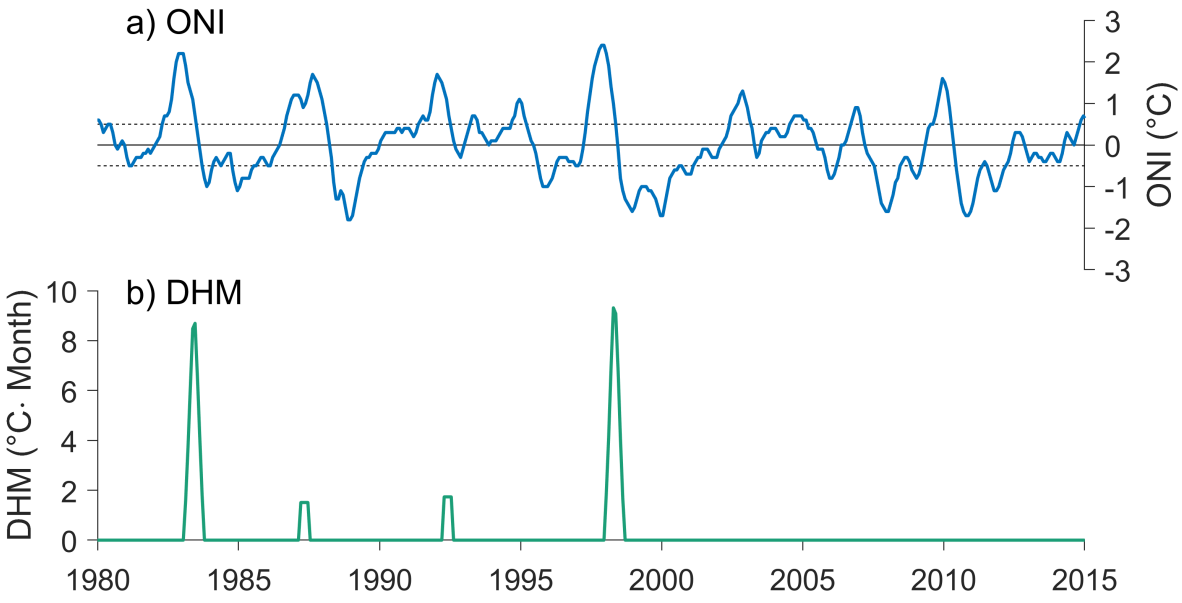

Figure S4. a) Oceanic Niño Index and b) Degrees Heating Month from 1980 to 2015. The dashed lines indicate ±0.5°C, the threshold commonly used to define El Niño and La Niña events.

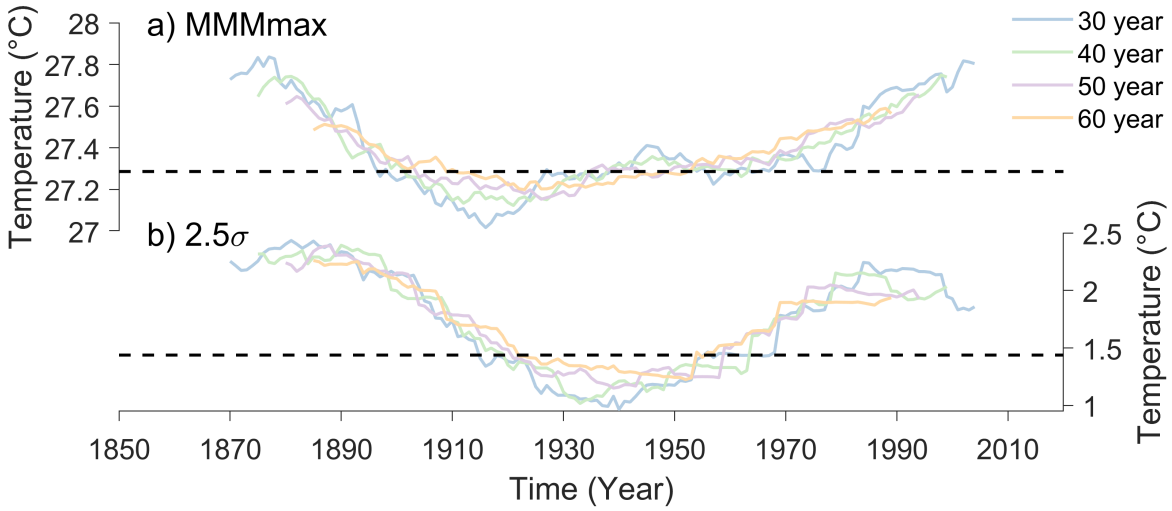

Figure S5. Running values of a) Mean maximum monthly SST and b) 2.5 standard deviation of mean maximum monthly SST with different window lengths (blue = 30 year, green = 40 year, purple = 50 year, orange = 60 year). The dashed lines indicate the values used in this current study.

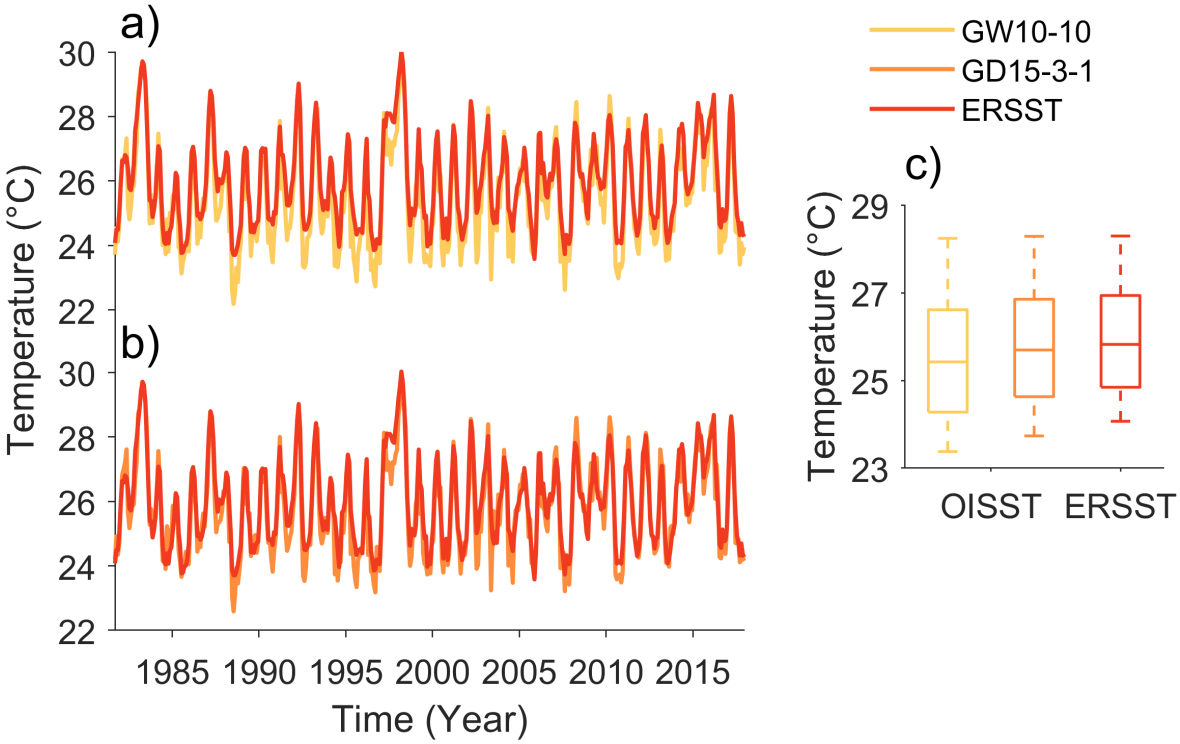

Figure S6. Comparison of SST from OISST and ERSST at a) Wolf and b) Darwin. c) SST distribution based on each product at each site. Due to the coarser resolution of ERSST, one grid-square represents both Wolf and Darwin (red); the orange and yellow series represent OISST from Darwin and Wolf, respectively. Whiskers represent the 5^{th} and 95^{th} percentile of the distributions.

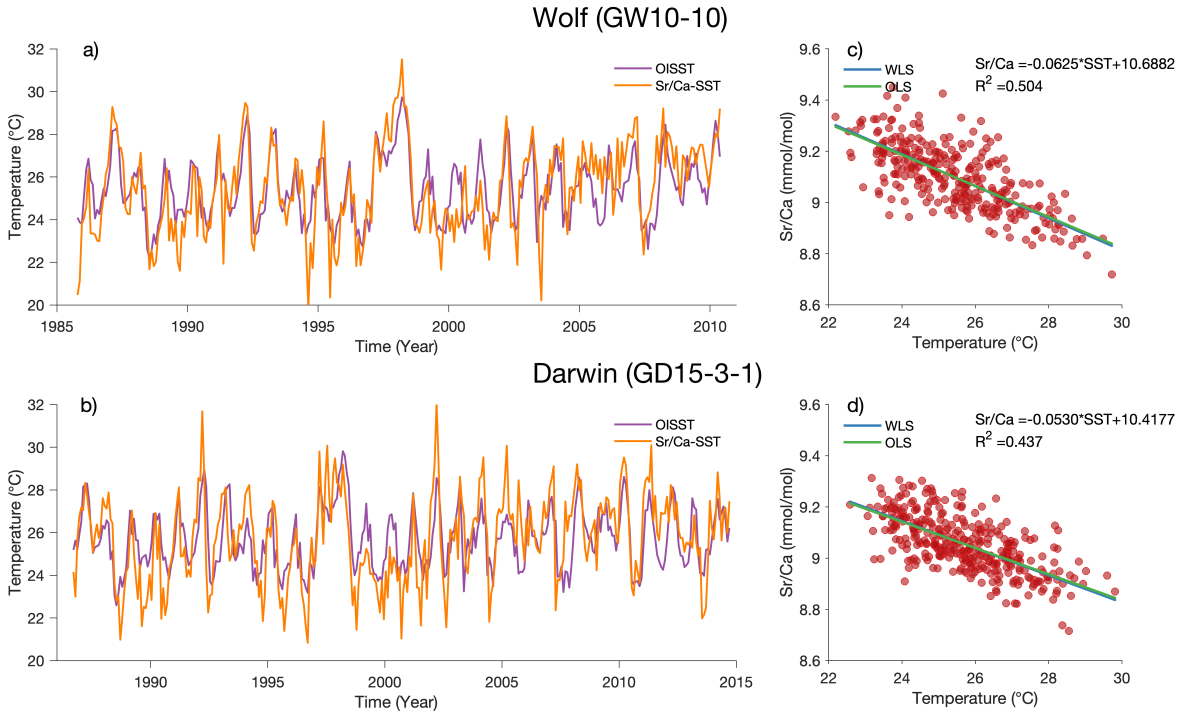

Figure S7. Monthly Sr/Ca and SST relationship. Time series of instrumental SST and Sr/Ca inferred SST from a) GW10-10 and b) GD15-3-1. Also shown are Sr/Ca regressed onto SST for c) GW10-10 and d) GD15-3-1, with equations for weighted least squares regressions.

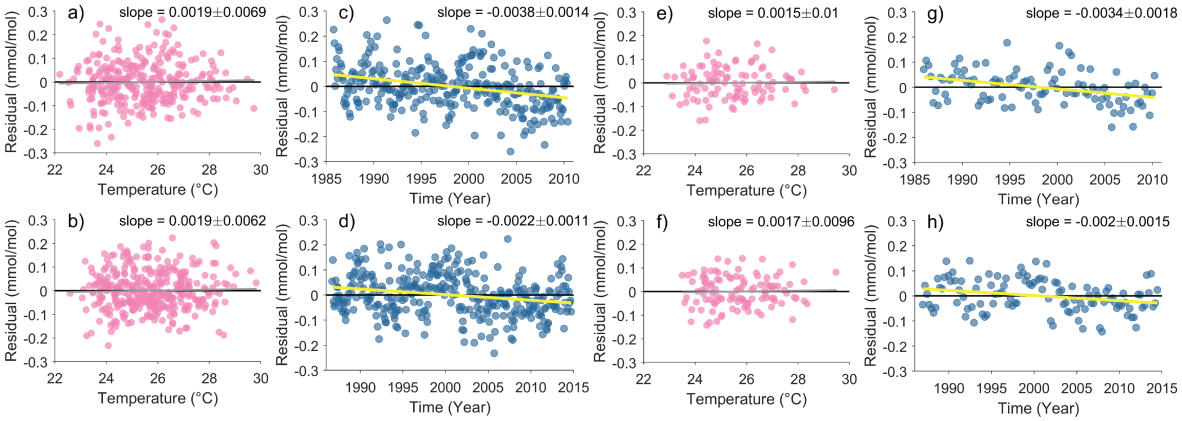

Figure S8. Residual characteristics from Sr/Ca calibration at monthly resolution: a-b) Relationship between residuals and temperature and c-d) the residual trend based on monthly data. Seasonal (3-month) resolution: e-f) Relationship between residuals and temperature and g-h) the residual trend based on 3-month data. Top row are results from GW10-10; bottom row are results from GD15-3-1. Also shown are regression slopes with the 95% confidence interval

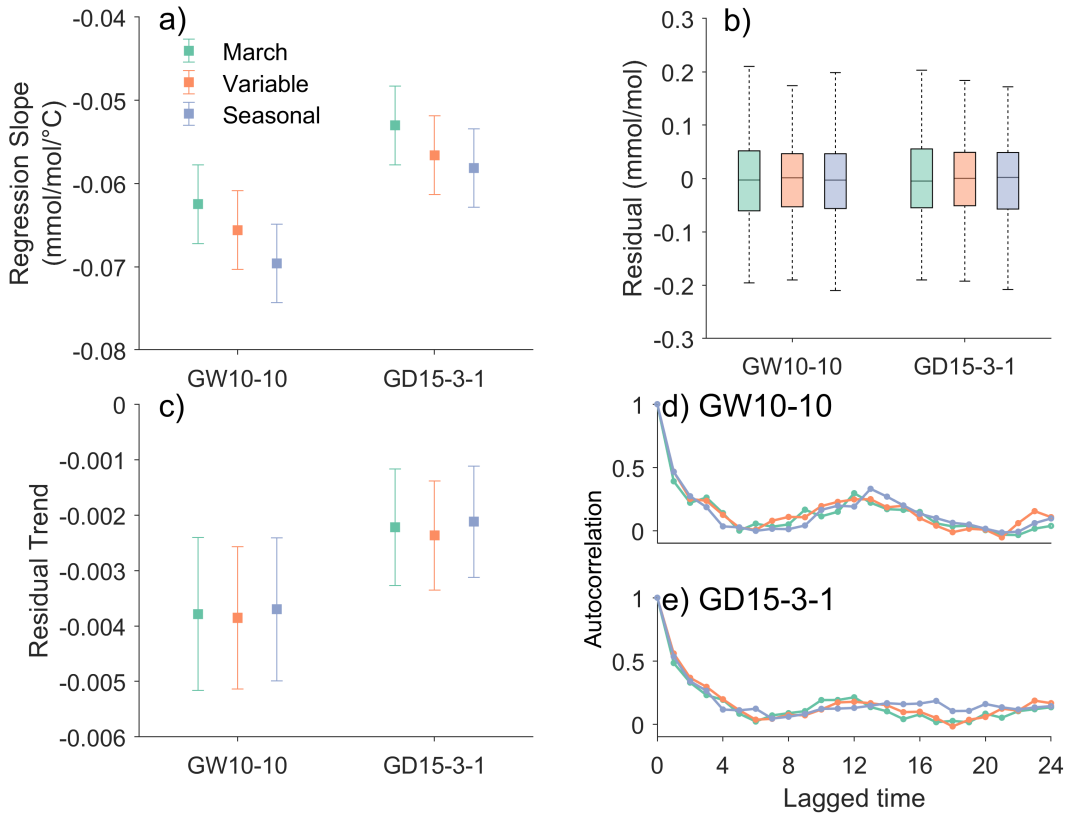

Figure S9. Regression slopes and residual characteristics using three age model strategies. a) Regression slope of Sr/Ca-SST using WLS, b) residual distribution, c) residual trend through time, and autocorrelation functions of d) GW10-10 and e) GD15-3-1. Green represents results from the original age model, orange represents results from the age model where Sr/Ca minima was tied to observed month of SST maxima, purple represents from the age model where Sr/Ca minima and maxima were tied to observed months of SST maxima and minima respectively.

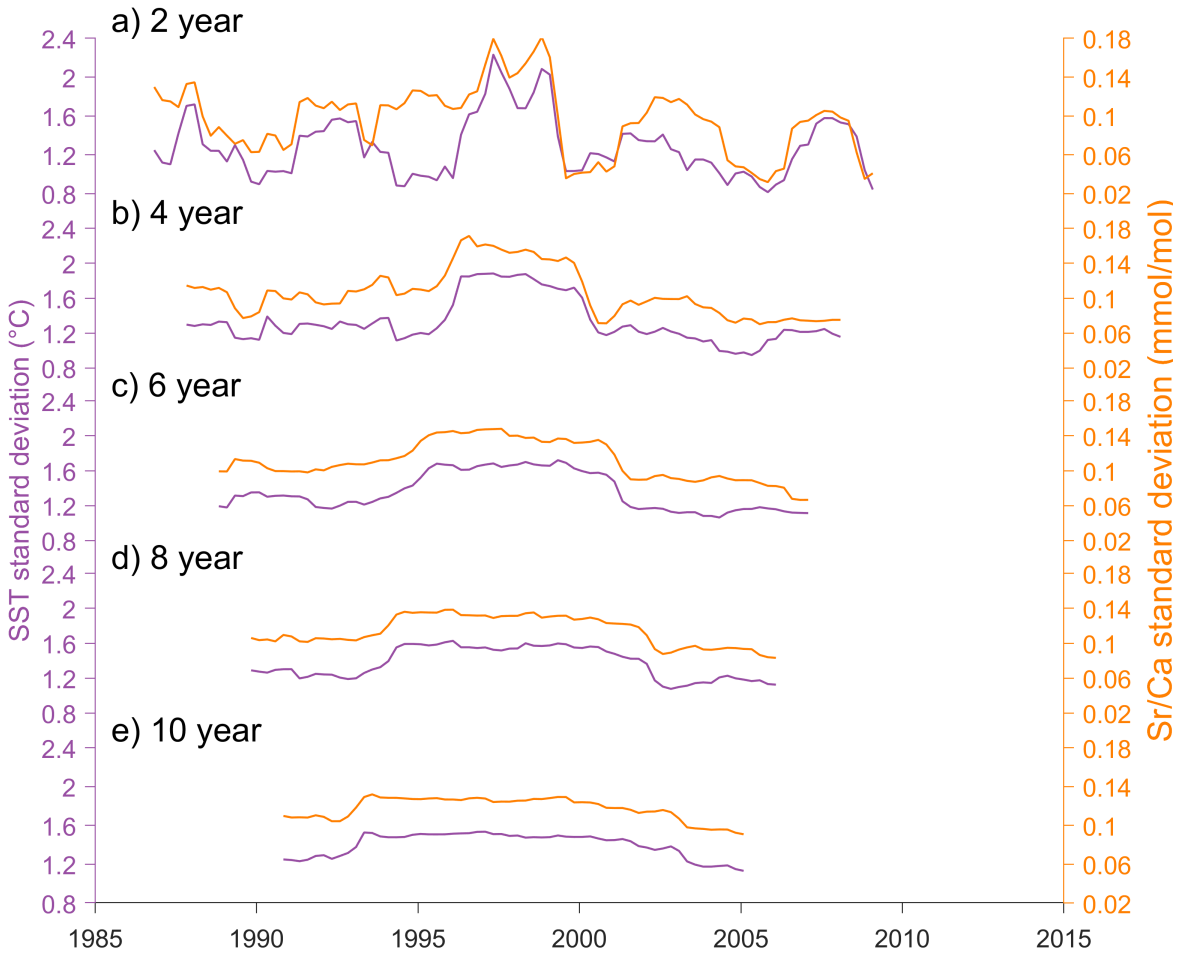

Figure S10. Running standard deviation of GW10-10 Sr/Ca (orange) and OISST (purple) using 3-month averaged data, calculated over a) 2 year, b) 4 year, c) 6 year, d) 8 year, e) 10 year running windows.

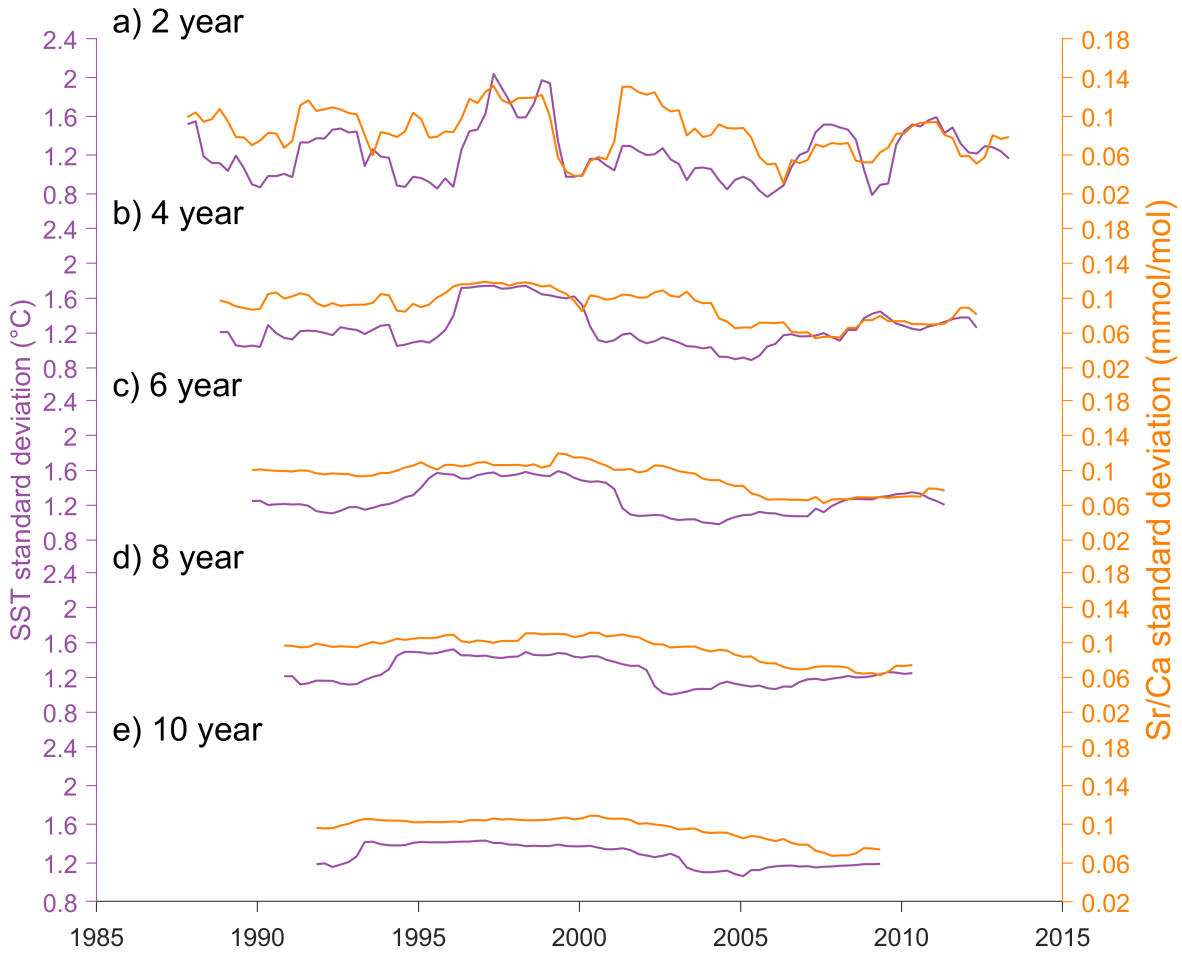

Figure S11. Running standard deviation of GD15-3-1 Sr/Ca (orange) and OISST (purple) using 3 month averaged data, calculated over a) 2 year, b) 4 year, c) 6 year, d) 8 year, e) 10 year running windows.

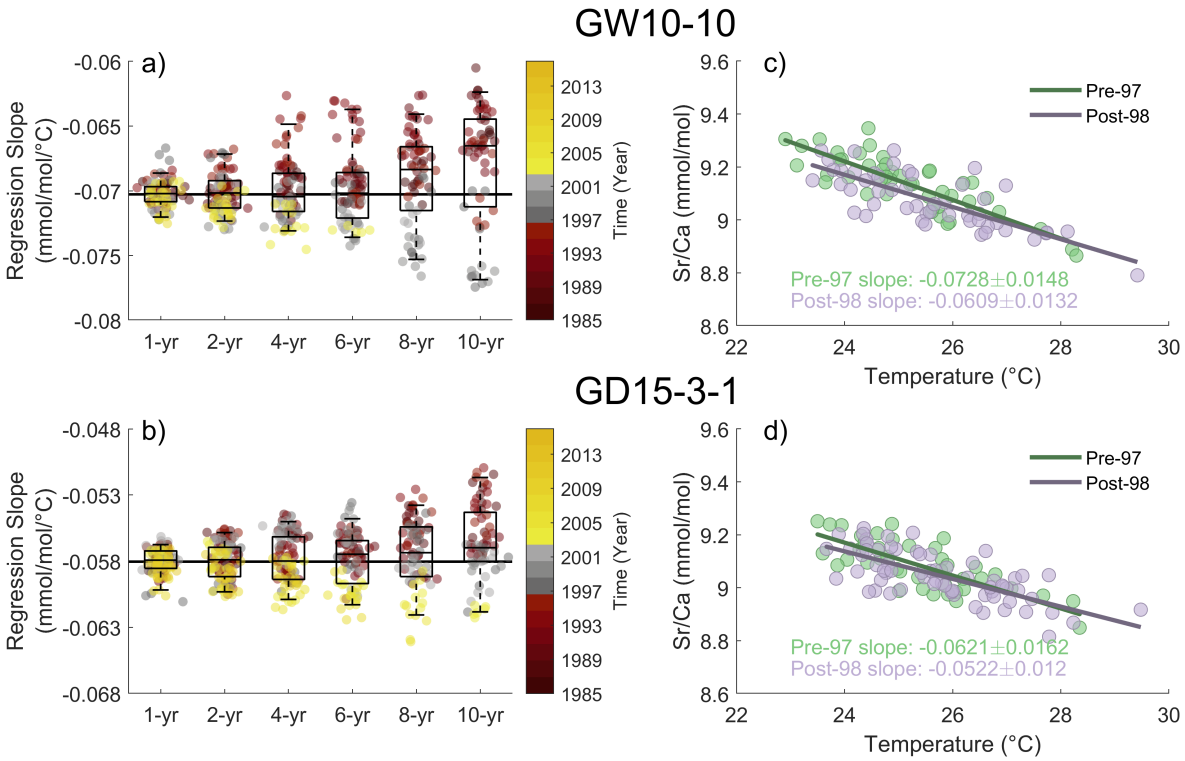

Figure S12. Regression slopes based on subsampling. a-b) regression slopes obtained from Sr/Ca and SST where a subset with different length (1, 2, 4, 6, 8, 10 years) was removed. The color represents the middle year of the data that was removed before the calibration. Solid black horizontal line indicates the weighted regression slope using the full dataset. c-d) Comparison between regression equations using data before 1997 and after 1998. Top panels show results from GW10-10 and bottom show results from GD15-3-1, using 3-month averages in each.

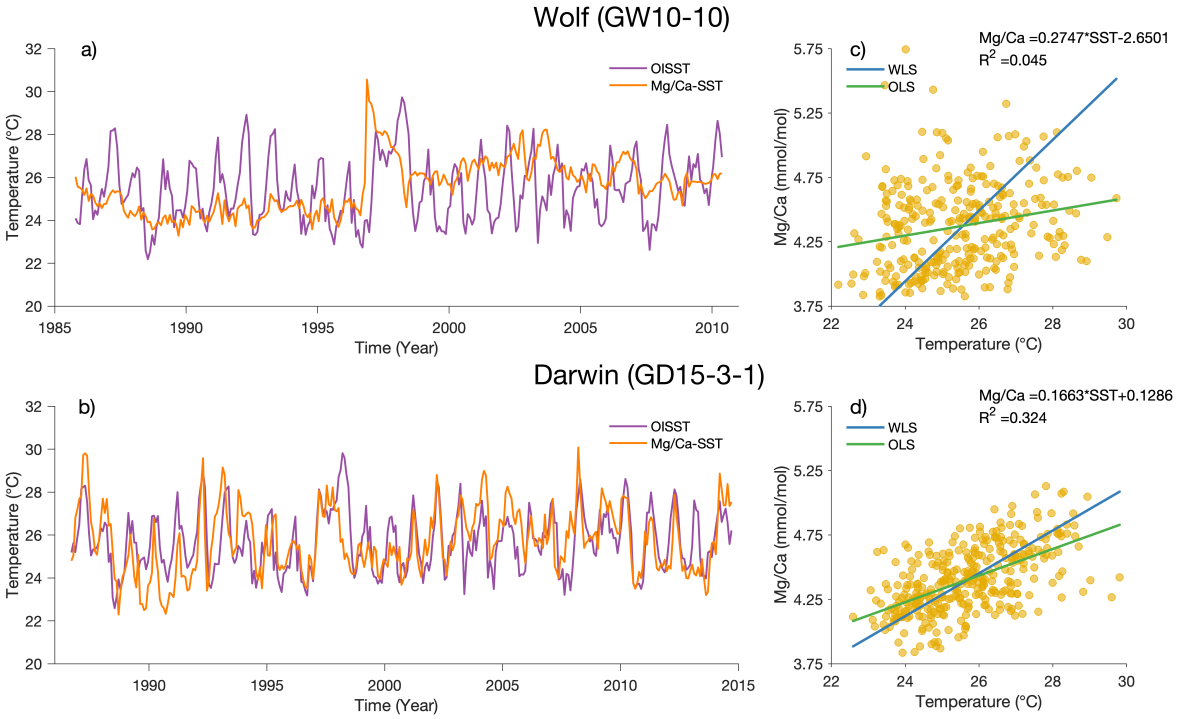

Figure S13. Monthly Mg/Ca-SST relationship. Time series of instrumental SST (purple) and Mg/Ca-inferred SST (orange) from a) GW10-10 and b) GD15-3-1. Also shown are Mg/Ca regressed onto SST for c) GW10-10 and d) GD15-3-1, with equations for weighted least squares regressions.

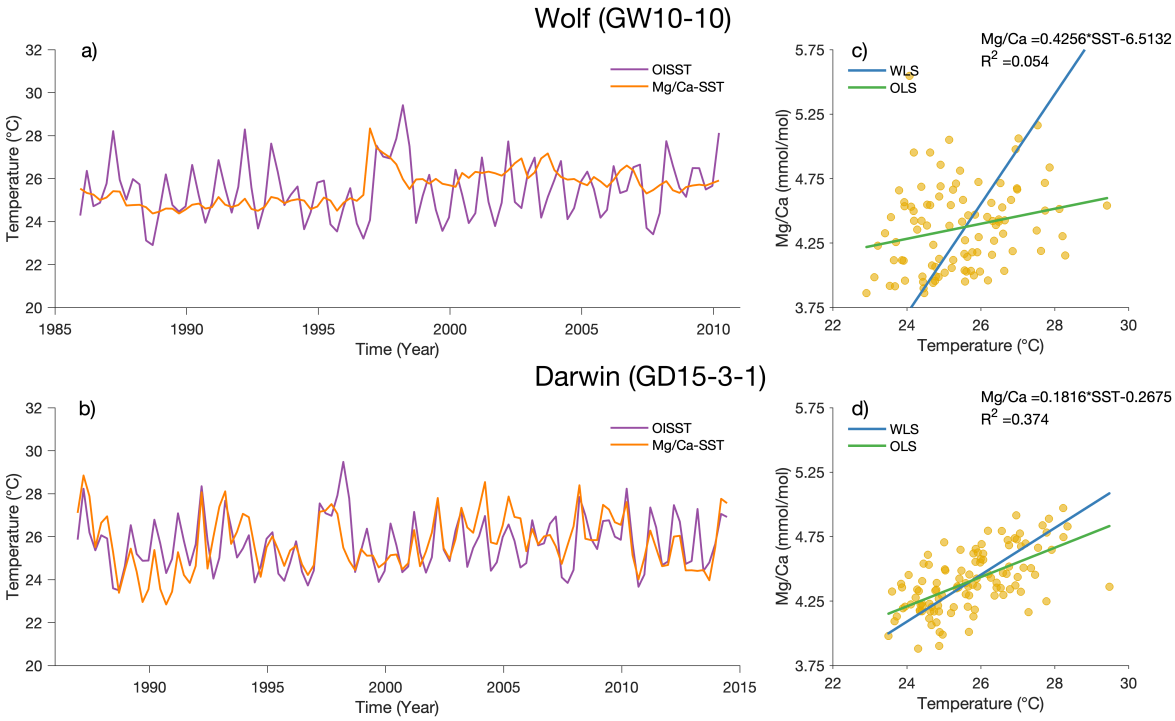

Figure S14. Seasonal Mg/Ca and SST relationship. Time series of instrumental SST and Mg/Ca inferred SST from a) GW10-10 and b) GD15-3-1. Also shown are Mg/Ca regressed onto SST for c) GW10-10 and d) GD15-3-1, with equations for weighted least squares regressions.